LAND SURFACE TEMPERATURE RESPONSES TO VEGETATION AND SOIL MOISTURE INDEX USING LANDSAT-8 DATA IN LUONG SON DISTRICT, HOA BINH PROVINCE

Vo Dai Nguyen[1], Nguyen Hai Hoa[1*], Nguyen Quyet[1], Pham Duy Quang[1]
[1]*Vietnam National University of Forestry*

SUMMARY

Land surface temperature (LST) is considered as a key factor in natural processes. Remote sensing data, including Landsat-8 data, offers numerous opportunities to better understand the land processes. This study has conducted to construct land use and land cover map in 2020 using NDVI thresholds. The study then calculated the LST, NSMI, NDBI and Slope of Luong Son district, Hoa Binh province using Landsat-8 OLI/TIRS data. Models showing the relationships between the LST and independent variables (NDVI, NSMI, NDBI and Slope) were developed using R statistical software. As a result, NDVI used for land use and land cover mapping is confirmed with the overall accuracy assessments of 92.0% and Kappa coefficient of 0.85. Study developed 37 linear regression models, one of them was selected and used to predict the LST in Luong Son district. The selected model ($R^2 > 0.60$, $P_{value} < 0.0001$) confirms that an increase of built-up land (NDBI) and loss of vegetation cover (NDVI) become a serious threat to the increase in land surface temperature in Luong Son district. This study implies that an increase of vegetation cover would lead to a slight decrease in land surface temperature, and built-up land expansion would be one of main responsible drivers for an increase of the LST. The only way to mitigate this risk is to increase additional vegetation cover in the built-up land; to both protect the existing forests and promote afforestation activities, which can considerably reduce the land surface temperature.

Keywords: land surface temperature, Landsat data, NDBI, NDVI, NSMI, regression model.

1. INTRODUCTION

As defined by Anandababu et al. (2008) land surface temperature is the surface temperature of the earth's crust where the heat and radiation from the sun are absorbed, reflected and refracted. It is considered as one of the most important aspects of land surface. Many fields, such as global climate change, hydrological, geo-/biophysical, and urban land use/land cover, rely heavily on land surface temperature (Rajeshwari and Mani, 2014). Therefore, changes in land use land cover or vegetation cover is relatively sensitive to the land surface temperature. Plants are known as a primary factor influencing the water balance of soil in natural and building ecosystems by changing the transfer of heat and moisture from the soil surface to the air (Acharya et al., 2016). Soil moisture links with land surface temperature through the water cycle, which in turn influences plant development (Malo and Nicholson, 1990). Artificial impermeable surfaces (sealed soils) cause heat storage to increase during the day and release to be slower at night, resulting in a greater land surface temperature than green areas (Morabito et al., 2016). The impact of topography on the LST varies depending on the quantity of solar energy received, and the impact of topography on the LST changes through time. There is a great difference in the land surface temperature among different types of land use (Xiao and Weng, 2007). Along with that, Kumar and Shekhar (2015) concluded the distribution of land surface temperature (LST) is significantly influenced by vegetation coverage. Pablos et al. (2016) identified that land surface temperature regulation is strongly influenced by the energy balance extension of soil moisture, an important component of the Earth's surface water balance. Adulkongkaew et al. (2020) indicated that in recent years, LST has tended to increase in both urban and suburban areas. Peng et al. (2020) pointed out that topography, especially slope is an important factor in controlling LST.

Luong Son district is located in Hoa Binh province, a mountainous province of Vietnam, located in the nation's Northwest region, with 298,103 ha of forest areas and 64.66% of provincial coverage. In Hoa Binh, recent records have showed that the highest temperature in summer could reach 34^0C and the lowest temperature in January can be around 12.9^0C, but with very high humidity, it causes chilling phenomenon (Luong Son Gov, 2016). Changes in climatic factors like as land surface temperature often lead to changes in vegetation cover in certain locations. In addition, due to the shortage of investigation and studies in the correlation between land surface temperature with vegetation, built-up area and soil

**Corresponding author: hoanh@vnuf.edu.vn*

moisture, there are still a few comprehensive documents and information about vegetation, temperature, soil moisture and their relationship in this study site.

Advanced spatial analysis tools and remote sensing technologies have been developed rapidly over the past decades. They offer a series of sensors that can operate at a variety of imaging scales (Rogan and Chen., 2004; Hoa et al., 2020). The climate effect on regional ecosystems can be demonstrated by the response of vegetation covers to climatic characteristics with the application of remote sensing (Carlson, 2000). LST measures the emission of thermal radiance from the land surface where the incoming solar energy interacts with and heats the ground, or the surface of the canopy in vegetated areas (Ansar, 2021). The normalized difference vegetation index (NDVI) has been used extensively in remote sensing studies (Seaquist, 2003). Besides, NDVI is a widely used indicator for tracking vegetation dynamics and land surface responses to hydrological variations at large scales (Ahmed et al., 2017). Similarly, the NSMI represents a dimensionless parameter that can be used to quantify gravimetric soil moisture (Haubrock et al., 2008; Alonso et al., 2019). The normalized difference built-up index (NDBI) has been useful for mapping urban buildup areas using Landsat Thematic Mapper (TM) data (Bhatti and Tripathi, 2014). Slope is a useful parameter to assess changes in LST. On worldwide scale, many studies have evaluated the relationship between LST with NDVI, NDBI, NSMI and slope (Kim, H. J et al., 2014; Chi, et al., 2020).

The main objective of the study was to analyses the relationships between land surface temperature (LST) and independent variables (NDVI, NSMI, NDBI, and Slope). To do this, land use and land cover in 2020 was created using Landsat-8 (2020). It then calculated NDVI, NSMI, NDBI and Slope for modelling development. Multiple linear regression models have been developed to identify the predictor and it's for the LST in Luong Son district. Finally, the selected models would be useful to understand how much the LST changes when the NDVI, NSMI, NDBI, and Slope change. These findings would be also important to imply how to maintain vegetation covers in Luong Son District.

2. RESEARCH METHODOLOGY

2.1. Study site

The study site of Luong Son district, Hoa Binh province is located in the Northwest parts of Vietnam. Hoa Binh province. It lies between $105^0$25'14" ÷ $105^0$41'25 E; and $20^0$36'30" ÷ $20^0$57'22" N (Fig. 1). It borders with Ky Son district in the West. The South borders on the Districts of Kim Boi and Lac Thuy. The East borders on My Duc and Chuong My districts (Hanoi city); the North borders Quoc Oai district (Hanoi City).

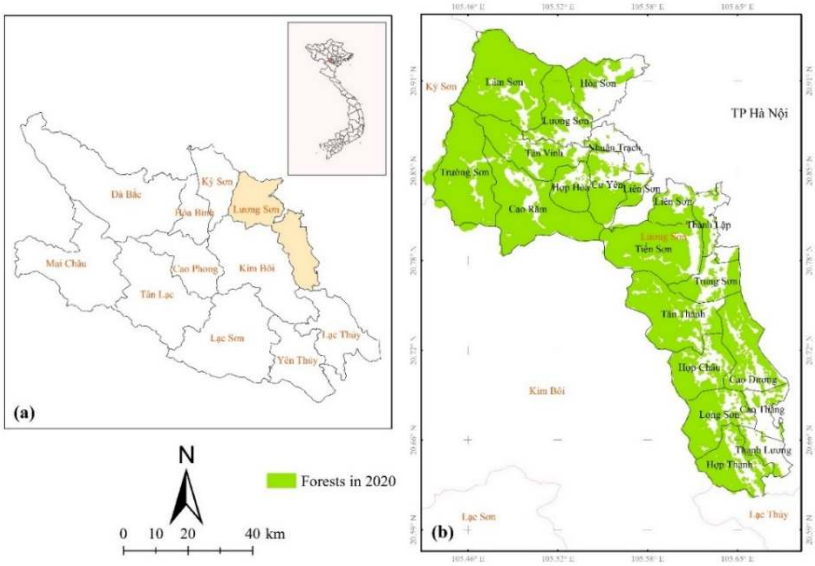

Fig. 1. Study site: (a) Geographic location of Luong Son district, Hoa Binh province; (a) Luong Son district as study site

Luong Son district has the advantage of geographical position, being a hub for economic, cultural and social exchange between the Northwestern mountainous region and the Red River Delta region. The total natural areas of the Chuong My district is estimated 36,488.85 ha (Luong Son Gov, 2016). In terms of topography, Luong Son district belongs to the midland mountainous region, the transition between the plain and the mountainous region, so the terrain is diverse. The terrain is mountainous with an altitude of about 200 - 400m. The population of the district is about 98,856 people, including 3 main ethnic groups, namely Muong, Dao, and Kinh (Luong Son Gov, 2016). This study is one of the hottest histrict of Hoa Binh in summer because it is surrounded by mountains. The detection of the extent of land surface temperature and its relationships with other associated drivers would be useful for adopting mitigation measures in a changing climate.

2.2. Methods

2.2.1. Remote sensing data

In this study, Landsat-8 data in 2016 and 2020 were freely downloaded as shown in Table 1. Landsat-8 data (2016 and 2020) were both used to construct land use and land cover maps based the defined thresholds of each land cover type in the Luong Son district. The Landsat-8 data in 2020 was used to develop the models showing the relationships between LST (Land Surface Temperature) and NDVI (Normalised Difference Vegetation Index), NDBI (Normalised Difference Built-up Index), NSMI (Normalised Soil Moisture Index), and Slope in Luong Son district, Hoa Binh province. These indices are commonly used in previous studies in relation to land use and land cover mapping (Schnur et al., 2010; Chuai et al., 2013).

Table 1. Remotely sensing data used this study

No	Image codes	Date	Spatial resolution (m)
1	LC08_127046_20200628_20200824_02_T1	28/06/2020	30
2	DEM	11/02/2000	30
3	Forest status map	2020	1:50.000

Source: https://earthexplorer.usgs.gov; [1]Hoa Binh Forest Protection Department (2021).

2.2.2. Image processing and indices calculation

Landsat-8 data pre-processing: As the Landsat-8 data (2020) was successfully downloaded, all of the pre-processing procedures of Landsat-8 (2020) was undertaken based on the guideline of Landsat preprocessing methods (e.g. Padro et al., 2017; Shimizu et al., 2018; Afrin, et al., 2019). In this study, the pre-processing procedures included radiometric correction, atmospheric correction, topographic correction, subset, bands combination (composite bands). In particular, Landsat-8 OLI/TIRS data are subjected to several corrections, such as radiometric and atmospheric issues. Landsat-8 data (2020) were converted to surface reflectance by top-of-atmosphere (TOA) method using ArcGIS 10.4.1. Thermal atmospheric correction was performed on TIR bands with normalized pixel regression method. Radiometric correction was done to reduce and correct errors in the digital numbers of images. This process would improve the interpretability and quality of remotely sensed Landsat-8 data. Radiometric calibration and correction are particularly important as comparing data sets over a multiple time period. Radiometric calibration was also applied this study as a sensor records the intensity of electromagnetic radiation for each pixel known as digital number (DN). These digital numbers were converted to more meaningful real world units, such as radiance, reflectance or brightness temperature. Sensor specific information obtained from Landsat-8 data as the metadata file was needed to carry out this calibration. Radiometric calibration of Landsat-8 data (2020) was converted directly to reflectance using ArcGIS 10.4.1. Similarly, atmospheric correction was applied to remove the effects of the atmosphere and produce surface reflectance values. Atmospheric correction also significantly enables improve the interpretability and use of Landsat-8 data. Other preprocessing procedures were applied as the studies of Song et al., (2001); Hai-Hoa et al., (2020).

Normalized Different Vegetation Index calculated (NDVI):

One of the most commonly interpretation methods for land use and land cover is based on

the values of NDVI. In this study, we used the NDVI thresholds to classify NDVI into different classes (Mohajane et al., 2018). Mohajane et al., (2018) has used NDVI threshold values for three vegetation categories as NDVI values below to 0.2 are considered as low-density vegetation; NDVI values between 0.2 and 0.5 are moderate-density vegetation and NDVI values higher than 0.5 are high-density vegetation. However, we would define the NDVI threshold values for three land covers, namely water, non-forest and forest classes in the study site. In general, NDVI values range from -1 to 1. The highest value represents healthy vegetation, while the lowest NDVI value shows non-vegetation cover (Sellers et al., 1992; Mavi and Tupper, 2004). Non-vegetation cover includes barren surfaces (rock and soil), water, snow, and ice, normally ranging near zero and decreasing negative values (Saravanan et al., 2019). The following formula of NDVI is presented as below (Schnur et al., 2010; Chuai et al., 2013):

$$\mathrm{NDVI} = \frac{\mathrm{Band_{NIR}} - \mathrm{Band_{RED}}}{\mathrm{Band_{NIR}} + \mathrm{Band_{RED}}}$$

For Landsat-8, Band-4 is the RED Band reflectance; and Band-5 is the NIR Band reflectance.

Normalized Soil Moisture Index calculated (NSMI):

Normalized Soil Moisture Index (NSMI) is defined as a non-dimensional measure of reflectance spectra, calculated from difference of the reflectance of two specific spectral bands, 1800 nm ÷ 2119 nm, using mathematical operations (Haubrock et al., 2008). The efficiency of the environment compensation processing has a significant impact on NSMI results (Fabre et al., 2015). This study used NSMI to measure the soil moisture and quantify the gravimetric soil moisture (Dinh et al., 2019). The NSMI was straightforward to use and interpret (Nocita et al., 2013; Hong et al., 2017). The formula of NSMI in Landsat-8 was designed and followed the study of Fabre's work (2015) as shown below:

$$\mathrm{NSMI} = \frac{\mathrm{Band_{SWIR1}} - \mathrm{Band_{SWIR2}}}{\mathrm{Band_{SWIR1}} + \mathrm{Band_{SWIR2}}}$$

For Landsat-8, Band-6 is the SWIR1 Band reflectance; and Band-7 is the SWIR2 Band reflectance.

Normalized Difference Built-up Index calculated (NDBI):

NDBI is one of the significant indices applied widely to identify the built-up information and to extract the built-up land use. The formula is indicated as below.

$$\mathrm{NDBI} = \frac{\mathrm{Band_{SWIR1}} - \mathrm{Band_{NIR}}}{\mathrm{Band_{SWIR1}} + \mathrm{Band_{NIR}}}$$

For Landsat-8, Band-6 is the SWIR1 Band reflectance; and Band-5 is the NIR Band reflectance.

NDBI value lies between -1 ÷ 1. The negative value of NDBI represents water bodies, while higher value indicates built-up areas. NDBI value for vegetation is low.

Slope values calculated from 2011 DEM (30m, unit degree):

DEM (Digital Elevation Model) from ASTER remote sensing data has been used to calculate the slope of Luong Son District with the help of ArcGIS 10.4.1 software. The download DEM has implemented through pre-processing of extracting by mask tools to delineate the Luong Son region. Finally, the slope map of Luong Son district was created.

Land Surface Temperature calculated (LST):

Land Surface Temperature (LST) is known as a crucial index of remote sensing, which is used to estimate the temperature of surface cover and its surrounding environment. This parameter is widely used in land use and land cover change monitoring (LULC) (e.g. Bharath et al., 2013; Bokaie et al., 2016; Jiang and Tian, 2010;). LST is retrieved from thermal infrared (TIR) spectral measurements made by ground-based, airborne, or satellite-based sensors (Mutibwa et al., 2015). Therefore, it is necessary to convert the value of this digital image data into a spectral irradiance value that reflects the energy emitted by each object captured on the heat channel. Although there are two TIR spectral bands in Landsat-8 (Bands 10 and 11), we only used Band-10 this study due to being more stable than Band-11 and less difference from the monitored LST at weather station (Xu, 2015). The key steps of LST calculation were followed and summarised as below according to studies of Jeevalakshimi et al., (2017); Meng et al., (2019).

+ Digital number (DN) was converted to spectral radiance (Lλ) as below:

$$L\lambda = ML * Qcal + AL$$

Where: ML is Band-specific multiplicative rescaling factor from the metadata (radiance Mult_Band_x, where x is the band number);

AL is Band-specific additive rescaling factor from the metadata (Radiance_add_band_x, where x is the band number);

Qcal is Quantized and calibrated standard product pixel values (DN).

+ The next step was conversion to at-satellite brightness temperature as the following:

$$T = K_2/\ln((K_1/L\lambda) +1) -272.15$$

Where: T is At-satellite Brightness Temperature (K);

$L\lambda$ is TOA spectral radiance (Watts/m^2 srad * πm);

K_1 is Band-specific thermal conversion constant form the metadata (K_1_constant_Band_x, where x is the band number 10);

K_2 is Band-specific thermal conversion constant from the metadata (K_2_constant_Band_x, where x is the band number 10). For band 10: K_1 is 774.89; K_2 is 1321.08.

+ Proportion of Vegetation (Pv) is the ratio of the vertical projection area of vegetation on the ground, including leaves, stalks, and branches to the overall vegetation area (Neinavaz et al., 2020) and this value was calculated by using NDVI (Wang et al., 2015; Agapiou et al., 2020). The formula of calculating Pv is shown below:

$$Pv = (NDVI - NDVImin/NDVImax - NDVImin)^2$$

+ Land Surface Emissivity (ε) is defined as the efficiency of transmitting thermal energy as thermal infrared (TIR) radiation across the surface into the atmosphere (Avdan and Jovanovska, 2016). It is a crucial factor to compute LST with high accuracy (Zhang et al., 2017). After calculating Pv, LSE is then derived by the following formula:

$$LSE = 0.004 * Pv +0.986$$

+ LST is finally estimated by the following formula:

$$LST=BT/1+ W*(BT/p) * Ln (LSE)$$

Where: BT is At-Satellite Temperature;

W is Wavelength of emitted radiance (11.5μm = Band 10);

p=h*c/s (1.438*10^2-34Js);

h: Plantck's constant (6.626*10^-23J/K);

s: Boltzmann constant (1.38*10^23J/K);

c: velocity of light (2.998*10^8 m/s).

2.2.3. Accuracy assessments of land use and land cover classification

The accuracy assessment is an important process for evaluating the result of post-classification as the user of land cover outputs needs to know how accurate the results is. To use the data correctly, we considered the minimum level of interpretation accuracy in land use and land cover map would be at least 85.0% as suggested by previous studies of Anderson (1976); Thomlinson et al., (1999); Foody (2002). Randomly selected sample points were used to quantitatively assess the land cover classification accuracy. Total sample points used for the classification accuracy estimation were 274 points, 174 points for forest class, 50 points for water class (rivers, lakes, other water bodies), and 50 points for non-forest class. The overall classification accuracy, producer's accuracy and Kappa statistics were then estimated for quantitative classification performance analysis (Tso, 2001; Foody, 2013).

2.2.4. Model development

Randomly, 224 points with a 30-m buffer (equivalent to 2826 m or 94 pixels), 174 of which are forest points and 50 points are non-forest areas, have been extracted from NDVI, NSMI, NDBI, Slope, and LST data through ArcGIS 10.4.1. The mean value of each 20-m buffered point was taken for model development purpose.

Multiple linear regression model with the stepwise approach has been developed to predict the variable for measuring land surface temperature with the help of R (Statistics Package for Social Science). Here, the land surface temperature (LST) was taken as a dependent variable. NDVI and NSMI were taken as independent variables for predicting the land surface temperature in Luong Son District. R is multiple correlation coefficients which are considered as a measure of the worth of the prediction of the dependent variables. The values are statistically analyzed for the creation of a model using multiple linear regression with the stepwise approach in R where Y is the dependent variable (LST), α is the intercept, $\beta_{1,2,3,..n}$ are regression coefficients of the independent variables, and $x_{1,2,3,...n}$ are independent variables (NDVI, NSMI, NDBI, Slope), which would be the predictor of the dependent variable.

$$Y = \alpha + \beta_1 x_1 + \beta_2 x_2 + \cdots + \beta_n x_n$$

3. RESULTS AND DISCUSSION

3.1. Land use and land cover in Luong Son district

Accuracy assessment of land use and land cover classification:

The classification accuracy was evaluated by the confusion matrix. The classified image showed an overall accuracy of 92.0% in 2020, with a Kappa statistic of 0.85 (Table 2). User's and producer's accuracies of individual classes for 2020 of land cover map are presented in Table 2, and indicate that all classes have user's and producer's accuracies higher than 85.5%, with exception of non-forests in producer's accuracy assessments. The classification accuracy of the results was assessed based on the field survey results, the sampling points focused on the un-surveyed areas. During accuracy assessments, mapping accuracies might be affected by several possible factors, including mixed-pixel issues, images taken at different time and cloud cover percentage (Hoa et al., 2020). This result confirms that the land cover map can be used to assess the relationships between LST, NDVI, NSMI, NDBI and Slope in Luong Son district.

Table 2. Accuracy assessments of land cover classified by NDVI in 2020

Image classified	GPS				
	Water	**Non-forests**	**Forests**	**Total**	**User's Accuracy (%)**
Water	48	2	0	50	96.0
Non-forests	1	49	0	50	98.0
Forests	0	20	180	200	90.0
Total	49	71	180	**300**	
Producer's Accuracy (%)	98.0	69.0	100.0		
Overall accuracy (%): 92.0; Kappa coefficient is 0.85					

NDVI land cover classification in 2020:

The results presented in Figs. 2 & 3, Table 3 reveal that the class of forests was the dominant NDVI land cover class in 2020. It covers approximately 89.82% of Luong Son's territory (Table 3).

As results indicated in Fig. 2, the NDVI values in Luong Son district range from -0.605 ÷ 0.874, the greater the NDVI value is, the denser the forest cover is (Xie et al., 2008; Singh et al., 2016). Combined with field survey data shows that the higher NDVI value (> 0.40) is classed as forest class, while with lower NDVI value (0 ÷ <0.40) is categorised as other class (including grasslands, agriculture, residential areas, and others); and negative NDVI value (-0.605 ÷ 0) is surface water. Based on the land cover classification, the study defined thresholds of land cover in Luong Son district as shown in Table 3. These thresholds for land cover in 2020 was then used to classify land cover in 2016.

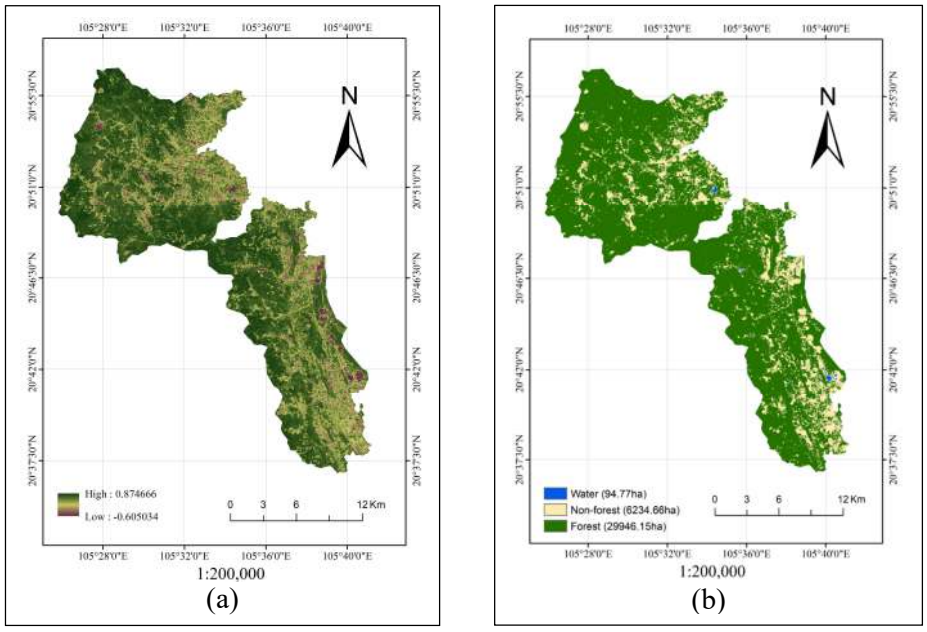

Fig. 2. NDVI values (a); Land use/cover in Luong Son district (Landsat-8 28/06/2020)

Table 3. NDVI thresholds for land covers classified in Luong Son district

Class	Water	Non-forests	Forests
NDVI	-0.605 ÷ 0.0	0.0 ÷ 0.5	0.4 ÷ 0.874
Areas in 2020 (ha)	94.8 (0.3%)	6234.7 (17.1%)	29946.2 (82.6%)

Table 3 shows that the total of forest areas in Luong Son district is estimated about 29946.2 ha (equivalent to 82.6%), while other land areas covered by non-forest areas (grassland, agricultural land, residential land, roads, bare land) are 6234.7 ha (17.1%). The land covered by water surface accounts for 94.8 ha (0.3%).

3.2. Land surface temperature, NSMI, NDBI and Slope in Luong Son district

Land surface temperature (LST):

Land surface temperature (LST) shows the mean temperature in forested areas and non-forested areas are 26.0^0C and 28.1^0C, respectively (Table 4), with a maximum temperature of 28.0^0C and minimum temperature of 22.2^0C for forested areas, a maximum temperature of 31.92^0C and minimum temperature of 25.24^0C for non-forested areas. Key statistics are summarised in Table 4.

Table 4. Summary of statistics of LST calculated from Landsat-8 in 2020

Land cover	Non-Forested areas					Forested areas				
Indices	**NDVI**	**NSMI**	**LST (^{0}C)**	**NDBI**	**Slope (º)**	**NDVI**	**NSMI**	**LST (^{0}C)**	**NDBI**	**Slope (º)**
Max	0.39	0.39	32.9	0.22	46.3	0.84	0.5	28.0	-0.14	51.3
Min	0.04	0.02	25.2	-0.62	0.0	0.56	0.29	22.0	-0.54	0.75
Mean	0.21	0.22	28.1	-0.16	8.82	0.76	0.43	26.0	-0.38	17.1
Std	8.7	7.81	1.66	0.2	10.5	7.74	3.22	1.1	5.44	8.46

As shown in Table 4, there is a difference in land surface temperature between non-forested and forested areas. Similarly, compared with non-forested area, the NSMI value and the LST is higher and lower in forested areas, respectively. Therefore, it can assume that high vegetation cover leads to high in NSMI value, lower vegetation cover results in lower NSMI value. In contrast, the higher vegetation cover is, the lower land surface temperature is and in turn.

NDBI, NSMI and Slope calculation:

NDBI, NSMI and Slope indicates that there are differences in mean NDBI, NSMI and Slope between non-forested areas and forested areas (Fig. 3).

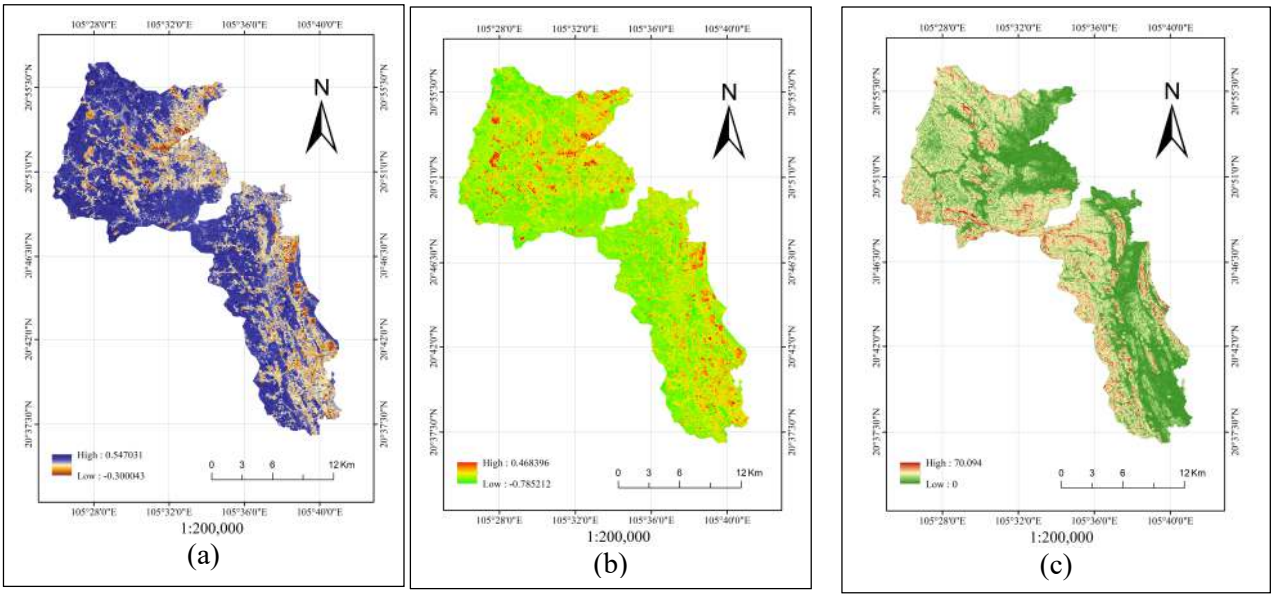

Fig. 3. Indices calculated from Landsat-8 28/06/2020: (a) NSMI values; (b) NDBI values; (c) Slope values in Luong Son district

In NDBI value, NDBI is used to map urban built-up areas with a range of -1.0 ÷ 1.0, the higher NDBI value indicate built-up areas and low value for vegetated areas. Indeed, high built-up areas land experiences high LST and low built-up land is evidenced with low LST (Table 4). Similarly, it clearly shows that where the region experiences high vegetation cover, the LST is less and vice versa. It is evidently there is a difference in max LST between non-forested and forested areas. Interestingly, there is a big difference in terms of soil moisture between non-forested (max NSMI =0.22) and forested areas (max NSMI = 0.43). Therefore, it assumes that both LST and vegetation cover are significantly influential factors in the moisture concentration in the soil. The LST has decreased from low elevated region to high elevated region. Vegetation increases the LST and these increases are indirectly proportional built-up land increases. Height (Slope) increases the temperature decreases. In short, built-up land plays a major role in increasing the temperature due to the hard concrete surface which contains almost nil water storage which leads to less humidity. The low humidity results in slow transpiration of the land surface. This process initiates the land surface temperature to increase easily.

3.3. Linear regression models between LST and other remote sensing indices

Linear regression models were developed to predict the variable for measuring land surface temperature (LST). In this study, the LST was taken as a dependent variable, while NDVI, NSMI, NDBI and Slope were taken as independent variables for predicting the LST of any given region either in Luong Son district or Hoa Binh province. As a result of linear regression model development, there are 37 models developed with a range of R^2 from 0.520 (Model 4) to 0.679 (Model 24), showing a moderate to good level of prediction (Table 5). The coefficient of determination is represented by R square (R^2) which indicates the proportion of variance in the dependent variables that can be explained by the independent variables. The R square values range from 0.520 (Model 4) to 0.679 (Model 37), so above 52.0% to 67.9% of the variation in the LST (dependent variable) can be explained by independent variables (NDVI, NDBI, NSMI, and Slope) shown in Table 5.

Overall, all of the models developed have P_{value} less than 0.001, known that the significant value of 0.00 is lesser than the alpha value of 0.05 indicating that the independent variables are statistically significant for the prediction of the dependent variable. This means that the adopted regression model is a good fit of the data.

Table 5. Summary of linear regression models developed: Relationships between LST and other predictor variables (NDVI, NSMI, NDBI, and Slope)

No	Models	R^2	P-values
1	LST = 31.1219 -12.8649*NSMI	0.593	<0.001
2	LST = 28.6096 + 10.6833 * (NDVI*NDBI)	0.571	<0.001
3	LST = 29.0423 + 8.7899*NDBI	0.538	<0.001
4	LST = 28.2990 + 21.3940 * (NDVI*NSMI*NDBI)	0.520	<0.001
5	LST = 29.7155 -2.7114*NDVI + 5.6510*NDBI	0.617	<0.001
6	LST = 30.6911- 8.8733*NSMI + 3.3502*NDBI	0.615	<0.001
7	LST = 29.0011 + 5.1910* NDBI + 11.2302*(NDVI*NSMI*NDBI)	0.592	<0.001
8	LST = 29.22536 + 7.54456*NDBI -0.05611*(NDVI*Slope)	0.589	<0.001
9	LST = 29.408515 + 8.626850*NDBI – 0.026590*Slope	0.559	<0.001
10	LST = 30.3071 -6.3792*NSMI + 29.6517*(NDVI*NDBI) -51.0336* (NDVI*NSMI*NDBI)	0.638	<0.001
11	LST = 28.7118 + 2.2904*NDVI + 45.3719*(NDVI*NDBI) - 64.1570*(NDVI*NSMI*NDBI)	0.637	<0.001
12	LST = 29.2300 + 2.2665*NDBI + 30.0626*(NDVI*NDBI) - 45.6457*(NDVI*NSMI*NDBI)	0.636	<0.001
13	LST = 30.43261 -6.98473*NSMI + 3.88784*NDBI -0.02834*(NDVI*Slope)	0.624	<0.001
14	LST = 29.65822 -2.17602*NDVI + 5.76245*NDBI – 0.02319*(NDVI*Slope)	0.622	<0.001
15	LST = 29.13557 + 4.61870*NDBI + 5.07468*(NDVI*NDBI) - 0.02753*(NDVI*Slope)	0.617	<0.001

No	Models	R^2	P-values
16	LST = 28.52729 + 5.92308*NDBI + 0.07238*Slope -0.14768*(NDVI*Slope)	0.614	<0.001
17	LST = 30.06768 -9.81049*NSMI + 0.06017*Slope -0.10138*(NDVI*Slope)	0.613	<0.001
18	LST = 28.00595 + 0.07736*Slope + 7.82381*(NDVI*NDBI) - 0.11994*(NDVI*Slope)	0.601	<0.001
19	LST = 27.64006 + 0.09801*Slope + 13.73126*(NDVI*NSMI*NDBI) - 0.15600*(NDVI*Slope)	0.574	<0.001
20	LST = 28.11218 -2.99723*NDVI +0.10290*Slope -0.16238*(NDVI*Slope)	0.548	<0.001
21	LST = 30.0387 +2.6185*NDVI -7.2186*NSMI + 37.0577*(NDVI*NDBI) - 57.6510*(NDVI*NSMI*NDBI)	0.651	<0.001
22	LST = 28.65176 + 2.79587*NDVI + 46.06276*(NDVI*NDBI) – 65.35218*(NDVI*NSMI*NDBI) -0.0295*(NDVI*Slope)	0.642	<0.001
23	LST = 28.62815 + 0.05115*Slope + 32.33102*(NDVI*NDBI) - 49.99425*(NDVI*NSMI*NDBI) -0.08218*(NDVI*Slope)	0.640	<0.001
24	LST = 29.73244 -5.63870*NSMI + 3.50655*NDBI + 0.07848*Slope - 0.09502*(NDVI*Slope)	0.634	<0.001
25	LST = 29.11828 -1.69397*NDVI +5.12580*NDBI + 0.04604*Slope - 0.08874*(NDVI*Slope)	0.631	<0.001
26	LST = 28.61134 + 3.92990*NDBI +0.05617*Slope + 4.08695*(NDVI*NDBI) -0.10416*(NDVI*Slope)	0.631	<0.001
27	LST = 28.55312 + 4.66898*NDBI + 0.06212*Slope + 5.75539*(NDVI*NSMI*NDBI) -0.11877*(NDVI*Slope)	0.624	<0.001
28	LST = 27.60047 + 1.91444*NDVI + 0.08433*Slope +10.92910*(NDVI*NDBI) -0.13731*(NDVI*Slope)	0.607	<0.001
29	LST = 30.38355 +1.99188*NDVI -10.61842*NSMI + 4.97372*(NDVI*NDBI) -0.02177*(NDVI*Slope)	0.606	<0.001
30	LST = 30.06208 +3.24387*NDVI -7.73492*NSMI +37.28577*(NDVI*NDBI) -58.60892*(NDVI*NSMI*NDBI) - 0.0295*(NDVI*Slope)	0.658	<0.001
31	LST = 30.0373 + 6.2742*NDVI -11.8112*NSMI -4.4552*NDBI +58.4370*(NDVI*NDBI) -86.8834*(NDVI*NSMI*NDBI)	0.657	<0.001
32	LST = 28.05976 +3.13874*NDVI +0.05851*Slope + 41.21894*(NDVI*NDBI) -57.73958*(NDVI*NSMI*NDBI) - 0.10482*(NDVI*Slope)	0.656	<0.001
33	LST = 28.85371 + 2.4682*NDBI +0.04431*Slope +24.18246*(NDVI*NDBI) -38.07884*(NDVI*NSMI*NDBI) -0.08144*(NDVI*Slope)	0.649	<0.001
34	LST = 29.72729 -5.24343*NSMI + 0.04085*Slope +26.48790*(NDVI*NDBI)	0.647	<0.001
35	LST = 29.33342 + 3.43672*NDVI -6.33340*NSMI +0.04676*Slope +35.00497*(NDVI*NDBI) -53.74683*(NDVI*NSMI*NDBI) - 0.09125*(NDVI*Slope)	0.666	<0.001
36	LST = 30.05994 +6.75755*NDVI -12.15768*NSMI -4.30651*NDBI + 57.94422*(NDVI*NDBI) -86.83502*(NDVI*NSMI*NDBI) - 0.02415*(NDVI*Slope)	0.664	<0.001
37	LST = 29.02306 +9.03602*NDVI -12.68862*NSMI -6.76316*NDBI +0.06646*Slope +66.48707*(NDVI*NDBI) - 96.02596*(NDVI*NSMI*NDBI) – 0.11792*(NDVI*Slope)	0.679	<0.001

a: dependent variable (LST, Land Surface temperature). b: predictors- constant, NDVI, NSMI, NDBI, and Slope.

As linear regression models shown in Table 5, the negative value of independent variables (NDVI, NSMI, NDBI, and Slope) indicates that the LST increase, which decreases in vegetation cover (NDVI, NDBI); soil moisture (NSMI) and Slope, so LST is negatively related to (NDVI, NSMI, NDBI) and slope and vice versa.

In general, all of the models developed can be used to predict the LST. However, this study would select one of shortlisted models in Table 5, which can be the best prediction of the LST in Luong Son district. To do this, some criteria have been taken into account: (1) the model should have $R^2 > 0.60$ at least; (2) P_{value} of the model and of each independent variable included in the model need be statistically significant with value less than 0.05; and (3) independent variables included in the model can

be easily and clearly explained to dependent variable (LST). As a result, the study has selected one optimal models for predicting the LST in Luong Son district (Table 6).

Table 6. Model summary of LST prediction in Luong Son district

1. Model 5:	**Estimate**	**Std. Error**	**t value**	**Pr(>|t|)**
(Intercept)	29.7155	0.2074	143.242	< 2e-16 ***
NDVI	-2.7114	0.4013	-6.757	1.23e-10 ***
NDBI	5.6510	0.6777	8.338	8.09e-15 ***

Signif. codes: 0 '***' 0.001 '**' 0.01 '*' 0.05 '.' 0.1 ' ' 1
Residual standard error: 1.02 on 221 degrees of freedom; Multiple R-squared: 0.6167, Adjusted R-squared: 0.6132; F-statistic:177.8 on 2 and 221 DF, p-value: < 2.2e-16; lm(formula = LST ~ NDVI + NDBI, data = LUONGSON)

As Table 6 shows the relationships between the LST and other independent variables (NDVI, NDBI). This study selected the Model 5 as the most suitable model for LST prediction in Luong Son district. As the Model 5 shows the LST is negatively and positively related to NDVI and NDBI, respectively. In other word, one unit decrease in the NDVI and one unit increase in the NDBI would be an increase of 32.7 units in the LST. Therefore, the Model 5 used to predict the LST from NDVI and NDBI is as follow: LST = 29.7155 – (2.7114 x NDVI) + (5.6510 x NDBI), R^2= 0.617.

4. CONCLUSION

The study concludes that Landsat-8 data is useful for estimating the LST, NDVI, and NDBI. NDVI used for land use and land cover mapping is reliable with the overall accuracy assessments of 92.0% and Kappa coefficient of 0.85. The high LST is recorded in Luong Son district where there are low vegetation cover and high built-up land. LST has indirect proportion to vegetation cover, but direct proportion to built-up land. The multiple regression model is very useful for the responsible predictor of land surface temperature (LST). The study has developed 37 linear regression models based on four parameters (NDVI, NSMI, NDBI, and slope). All of the developed models could be used to predict the LST in Luong Son district. However, the study finally selected the most suitable model which is best represented the relationships between the LST and NDVI and NDBI (Model 5, R^2 = 0.617) for Luong Son district.

The selected model confirms that an increase of built-up land (NDBI) and loss of vegetation cover (NDVI) become a serious threat to the increase in land surface temperature. The study also concludes that further parameters like rainfall, humidity, elevation included may improve the model. Vegetation plays a most significant role in mitigating the increasing land surface temperature, and built-up land expansion would be one of the main responsible drivers for the increase of land surface temperature. It suggests that it is very difficult to reduce the built-up land as the population has been growing. The only way to mitigate this risk is to increase additional vegetation cover in the built-up land; to both protect the existing forests and promote afforestation activities, which can considerably reduce the land surface temperature.

REFERENCES

1. Acharya, B.S., Hao, Y., Ochsner, T.E., Zou, C.B. (2016). Woody plant encroachment alters soil hydrological properties and reduces downward flux of water in tallgrass prairie. *Plant and Soil*. 1–13.

2. Adulkongkaew, T., Satapanajaru, T., Charoenhirunyingyos, S., Singhirunnusorn, W. (2020). Effect of land cover composition and building configuration on land surface temperature in an urban-sprawl city, case study in Bangkok Metropolitan Area, Thailand, *Heliyon 6* (2020) 04485

3. Afrin, A., Gupta, A., Farjad, B., Ahmed, M.R., Achari, G., Hassan, Q.K. (2019). Development of Land-use/Land-cover maps using Landsat-8 and MODIS data and their integration for hydro-ecological applications. *Sensors. 19:4891*.

4. Agapiou, A. (2020). Estimating Proportion of Vegetation Cover at the Vicinity of Archaeological Sites Using Sentinel-1 and -2 Data, Supplemented by Crowd sourced Open Street Map Geodata. *Appl. Sci.* 10, 4764.

5. Ahmed, M., Else, B., Eklundh, L., Ardö, J., Seaquist, J. (2017). Dynamic response of NDVI to soil

moisture variations during different hydrological regimes in the Sahel region, *Int. J. Remote Sens*.

6. Alonso, C., López, P., Benito, R.S., Tarquis, A.M. (2019). Correlation between vegetation index and soil moisture index using sentinel-2. *Estudios en la Zona No Saturada Del Suelo Vol. Xiv. Zns'19.*

7. Anandababu, D., Purushothaman, B. M., & Suresh, B. S. (2018). Estimation of land surface temperature using Landsat 8 data. *International Journal of Advance Research, Ideas and Innovations in Technology*, 4(2), 177-186.

9. Anderson, J. R., Hardy, E.E., Roach, J.T. and Witmer, R.E. (1976). A Land Use and Land Cover Classification System for Use with Remote Sensor Data. *Geological Survey Professional* Paper 964.

10. Ansar, K., Soumendu, C., Yupeng, W. (2021). Urban Heat Island Modeling for *Tropical Climates*. 978-0-12-819669-4.

11. Avdan, U., Jovanovska, G. (2016). Algorithm for automated mapping of land surface temperature using Landsat 8 satellite data. *Journal of Sensors*. 1– 8.

12. Bharath, S., Rajan, K.S., Ramachandra, T.V. (2013). Land surface temperature responses to land use land cover dynamics. *Geoinfor Geostat*. 54:50–78.

13. Bhatti, S. S. and Tripathi, N. K. (2014). Built-up area extraction using Landsat 8 OLI imagery. *GIS science Remote Sens*., vol. 51, no. 4, pp. 445–467, 2014.

14. Bokaie, M., Zarkesh, M.K., Arasteh, P.D., Hosseini, A. (2016). Assessment of Urban Heat Island based on the relationship between land surface temperature and Land Use/ Land Cover in Tehran. *Sustain Cities Soc.* 23:94–104

15. Carlson, T.N., Arthur, S.T. (2000). The impact of land use—land cover changes due to urbanization on surface microclimate and hydrology: a satellite perspective. *Global and Planetary Change*. 25(1–2):49–65.

16. Chi, Y., Sun, J., Sun, Y., Liu, S., Fu, Z. (2020). Multi-temporal characterization of land surface temperature and its relationships with normalized difference vegetation index and soil moisture content in the Yellow River Delta, China. *Global Ecology and Conservation*. 23, e01092.

17. Chuai, X.W., Huang, X.J., Wang, W.J., Bao, G. (2013). NDVI, temperature and precipitation changes and their relationship with different vegetation types during 1998–2007 in Inner Mongolia, China. *Int J Climatol*. 33:1696–706.

18. Dinh, N.T., Ha, N.T.T., Quy, D.T., Koike, K., Nhuan, M.T. (2019). Effective Band Ratio of Landsat 8 Images Based on VNIR-SWIR Reflectance Spectra of Top soils for Soil Moisture Mapping in a Tropical Region. *Remote Sens.* 11:716.

19. Fabre, S., Briottet, X., Lesaignoux, A., Avenue, B.P., Belin, E., Cedex, F.-T. (2015). Estimation of Soil Moisture Content from the Spectral Reflectance of Bare Soils in the 0.4–2.5 μm Domain. *Sensors* ISSN 3262–3281.

20. Foody, G. M. (2002) Status of land cover classification accuracy assessment. *Remote Sensing of Environment*. 80:185–201.

21. Foody, G.M. (2013). Ground reference data error and the mis-estimation of the area of land cover change as a function of its abundance. *Remote Sensing Letters*. 4:783-792.

22. Hai-Hoa, N., Lan, T.T.N., An, L.T., Nghia, N.H., Linh, D.V.K., Thu, N.H.T., Bohm, S., Premnath, C.F.S. (2020). Monitoring changes in coastal mangrove extents using multi-temporal satellite data in selected communes, Hai Phong city, Vietnam. *Forest and Society*. 4 256–70.

23. Hai-Hoa, N., Nghia, N. H., Nguyen, H. T. T., A. L. T., Lan, T. T. N., Linh, D. V. K., Furniss, M. J. (2020). Classification methods for mapping mangrove extents and drivers of change in Thanh Hoa province, Vietnam during 2005-2018. *Forest and Society*. 4, (1), 225–242.

24. Haubrock, S.N., Chabrillat, S., Lemmnitz, C., Kaufmann, H. (2008). Surface soil moisture quantification models from reflectance data under field conditions. *Int. J. Remote Sens*. 29, 3–29.

25. Hong, Y.S., Yu, L., Chen, Y.Y., Liu, Y. (2017). Prediction of soil organic matter by Vis-NIR spectroscopy using normalized soil moisture index as a proxy of soil moisture. *Remote Sens*. 10(1):28.

26. Jeevalakshmi, D., Narayana Reddy, S., Manikiam, B. (2017). Land surface temperature retrieval from LANDSAT data using emissivity estimation. *Int. J. Appl. Eng. Res*. 12:9679–9687.

27. Jeevalakshmi, D., Reddy, D.N., Manikiam, B., (2017). Land surface temperature retrieval from Landsat data using emissivity estimation. *International Journal of Applied Engineering Research* ISSN 0973- 4562 2(20): 9679- 9687.

28. Jiang, J., Tian, G. (2010). Analysis of the impact of Land use, land cover change on Land Surface Temperature with Remote Sensing. *Procedia Environmental Sciences*. 2:571–575.

29. Kim, H.J., Ryu, J.H., Seo, M.J., Lee, C.S.,Han, K.S. (2014). Approximate estimation of soil moisture from NDVI and land surface temperature over Andong region, Korean. *Korean Journal of Remote Sensing*. 30(3):375-381.

30. Kumar, D., Shekhar, S. (2015). Statistical analysis of land surface temperature-vegetation indexes relationship through thermal remote sensing. *Ecotoxicol Environ. Saf.* 121:39–44.

31. Luong Son Government. (2016). luongson.hoabinh.gov.vn

32. Malo, A., Nicholson, S., (1990). A study of rainfall and vegetation dynamics in the African Sahel using normalized difference vegetation index. *J. Arid Environ*. 19:1–24.

33. Mavi, H.S., Tupper, G.J. (2004). Agrometeorology: Principles and Application of Climate Studies in Agriculture. *Binghamton, NY, USA: Food Products Press*

34. Meng, X., Cheng, J., Zhao, S., Liu, S., Yao, Y. (2019). Estimating Land Surface Temperature from Landsat-8 Data using the NOAA JPSS Enterprise Algorithm. *Remote. Sens*. 11:155.

35. Meng, X., Zhao, J., Liu, S., Yao, Y., (2019). Estimating land surface temperature from Landsat-8 data using the NOAA JPSS enterprise Algorithm. *Remote Sensing*. 11:155. doi:10.3390/rs11020155

36. Mohajane, M., Essahlaoui, A., Oudija, F., Hafyani, M.E., Hmaidi, A.E., Ouali, A.E. (2018). Land use/land cover (LULC) using Landsat data series (MSS, TM, ETM+ and OLI) in Azrou Forest, in the Central Middle Atlas of Morocco. *Environments*. 5(12): 131-147.

37. Morabito, M., Crisci, A., Messeri, A., Orlandini, S., Raschi, A., Maracchi, G., Munafò, M. (2016). The impact of built-up surfaces on land surface temperatures in Italian urban areas. *Sci. Total Environ*. 551–552, 317–326.

38. Mutiibwa, D., Strachan, S., Albright, T. (2015). Land surface temperature and surface air temperature in complex terrain. *IEEE Journal of Selected Topics in Applied Earth Observations and Remote Sensing*. 8(10):4761–4774.

39. Neinavaz, E., Skidmore, A.K., Darvishzadeh, R. (2020). Effects of prediction accuracy of the proportion of vegetation cover on land surface emissivity and temperature using the NDVI threshold method. *Int. J. Appl. Earth Obs. Geoinf.* 85:1–13.

40. Nocita, M., Stevens, A., Noon, C., Van Wesemael, B. (2013). Prediction of soil organic carbon for different levels of soil moisture using VIS–NIR spectroscopy. *Geoderma*. 199:37–42.

41. Pablos, M., Martínez-Fernández, J., Piles, M., Sánchez, N., Vall-llossera, M., Camps, A. (2016). Multi-Temporal Evaluation of Soil Moisture and Land Surface Temperature Dynamics Using in Situ and Satellite Observations. *Remote Sens*. 2016, 8, 587.

42. Padró, J.C., Pons, X., Aragonés, D., Díaz-Delgado, R., García, D., Bustamante, J., Pesquer, L., Domingo-Marimon, C., González-Guerrero, O., Cristóbal, J., (2017). Radiometric Correction of Simultaneously Acquired Landsat-7/Landsat-8 and Sentinel-2A Imagery Using Pseudoinvariant Areas (PIA): Contributing to the Landsat Time Series Legacy. *Remote Sens*. 9:1319.

43. Rajeshwari, A. and Mani, N. (2014) Estimation of land surface temperature of dindigul district using landsat 8 data. *International Journal of Research in Engineering and Technology*, vol. 3, no. 5, pp. 122–126, 2014.

44. Rogan, J., Chen, D. (2004). Remote sensing technology for mapping and monitoring land-cover and land-use change. *Progress in planning*. 61(4):301-325.

45. Saravanan, S., Jegankumar, R., Selvaraj, A., Jacinth Jennifer, J., Parthasarathy, K.S.S. (2019). Utility of landsat data for assessing mangrove degradation in Muthupet Lagoon, South India. *Coastal Zone Management*. 471–484.

46. Schnur, M.T., Hongjie, X., Wang, X. (2010). Estimating root zone soil moisture at distant sites using MODIS NDVI and EVI in a semi-arid region of southwestern USA. *Ecol Inform*. 5:400–9.

47. Seaquist, J.W., Olsson, L., Ardö, J. (2003). A remote sensing-based primary production model for grassland biomes. *Ecological Modelling*. 169(1):131–155.

48. Sellers, P.J., Berry, J.A., Collatz, G.J., Field, C.B., Hall, G.F. (1992). Canopy reflectance, photosynthesis, and transpiration. III. A reanalysis using improved leaf models and a new canopy integration scheme. *Remote Sens Environ.* 42(3):187–216.

49. Shimizu, K., Ota, T., Mizoue, N., Yoshida, S., (2018). Assessments of preprocessing methods for Landsat time series images of mountainous forests in the tropics. *Journal of Forest Research*.

50. Singh, R.P., Singh, N., Singh, S., Mukheriee, S. (2016). Normalized Difference Vegetation Index (NDVI) based classification to assess the change in land use/land cover (LULC) in lower Assam, India. *International Journal of Advanced Remote Sensing and GIS*. 5(10):1963- 1970.

51. Song, C., Woodcock, C.E., Seto, K.C., Lenney, M.P., Macomber, S.A. (2001). Classification and Change Detection Using Landsat TM Data: When and How to Correct Atmospheric Effects? *Remote Sens. Environ*. 75: 230–244.

52. Thomlinson, J.R., Bolstad, P.V., Cohen, W.B. (1999). Coordinating methodologies for scaling land cover classifications from site-specific to global: steps toward validating global map products. *Remote Sensing of Environment*: 70:16 – 28.

53. Tso, B., Mather, P.M. (2001). Classification Methods for Remotely Sensed Data. London: Taylor & Francis. 2001.

54. Wang, T., Wedin, D.A., Franz, T.E., Hiller, J. (2015). Effect of vegetation on the temporal stability of soil moisture in grass-stabilized semi-arid sand dunes. *Journal of Hydrology*. 521:447–59.

55. Xiao, H., Weng, Q. (2007). The impact of land use and land cover changes on land surface temperature in a karstarea of China. *J. Environ. Manag*. 85(1):245–257

56. Xie, Y., Sha, Z., Yu, M. (2008). Remote sensing imagery in vegetation mapping: a review. *Journal of Plant Ecology*. 1(1):9- 23.

57. Xu, Hanqiu. (2015). Retrieval of the reflectance and land surface temperature of the newly-launched Landsat 8 satellite. *Chinese Journal of Geophysics*. 58:741-747.

58. Zhang, Y. Z., Jiang, X. G., Wu, H., Jiang, Y. Z., Liu Z. X., Cheng, H. (2017). Land Surface Temperature and Emissivity Separation from Cross-Track Infrared Sounder Data with Atmospheric Reanalysis Data and ISSTES Algorithm. *Advances in Meteorology*, vol. 2017, Article ID 7398312, 10 pages.

MỐI TƯƠNG QUAN GIỮA NHIỆT ĐỘ BỀ MẶT ĐẤT VỚI CHỈ SỐ THỰC VẬT VÀ ĐỘ ẨM ĐẤT BẰNG DỮ LIỆU ẢNH LANDSAT-8 TẠI HUYỆN LƯƠNG SƠN, TỈNH HOÀ BÌNH

Võ Đại Nguyên[1], Nguyễn Hải Hòa[1*], Nguyễn Quyết[1], Phạm Duy Quang[1]
[1]Trường Đại học Lâm nghiệp

TÓM TẮT

Nhiệt độ bề mặt đất (LST) là một trong những nhân tố sinh thái quan trong các quá trình sinh địa hoá tự nhiên. Dữ liệu viễn thám, bao gồm dữ liệu Landsat-8, cho phép chúng ta nghiên cứu và hiểu rõ hơn các quá trình trên một cách nhanh chóng và hiệu quả. Đề tài đã sử dụng dữ liệu Landsat-8 OLI/TIRS để xây dựng bản đồ sử dụng đất và độ che phủ đất 2020 bằng ngưỡng phân loại chỉ số NDVI, tính toán các chỉ số LST (nhiệt độ bề mặt đất), NSMI (chỉ số độ ẩm đất), NDVI (chỉ số thực vật), NDBI (chỉ số về khác biệt xây dựng) và độ dốc phục vụ việc xây dựng mô hình tương quan tại huyện Lương Sơn, tỉnh Hòa Bình. Các mô hình thể hiện mối quan hệ giữa LST và các biến độc lập (NDVI, NSMI, NDBI và Độ dốc) bằng phần mềm thống kê R. Kết quả đã xây 37 mô hình hồi quy tuyến tính thể hiện mối tương quan giữa LST với các chỉ số và độ dốc, trong đó mô hình 5 được lựa chọn và sử dụng để dự đoán LST tại huyện Lương Sơn. Mô hình được lựa chọn cho thấy sự gia tăng đất xây dựng (NDBI) và mất lớp phủ thực vật (NDVI) trở thành mối đe dọa nghiêm trọng đối với sự gia tăng nhiệt độ bề mặt đất ở huyện Lương Sơn. Kết quả của thấy mô hình cho thấy rằng sự gia tăng lớp phủ thực vật sẽ dẫn đến suy giảm nhiệt độ bề mặt đất và việc mở rộng đất xây dựng sẽ là một trong những nguyên nhân chính gây ra sự gia tăng LST. Giải pháp duy nhất để giảm thiểu rủi ro này là tăng cường lớp phủ thực vật bổ sung trong khu vực đô thị, dân cư; bảo vệ các diện tích rừng hiện có, thúc đẩy các hoạt động trồng rừng. Các giải pháp sẽ góp phần làm giảm đáng kể sự gia tăng nhiệt độ bề mặt đất.

Từ khóa: Landsat, mô hình, NDVI, NSMI, nhiệt độ bề mặt đất.

Received : 14/5/2021
Revised : 18/6/2021
Accepted : 25/6/2021